Highly Sensitive Naphthalimide-Based Fluorescence Polarization Probe for Detecting Cancer Cells

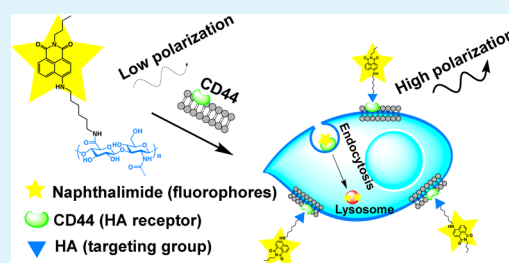Ti Jia, Congying Fu, Chusen Huang,* Haotian Yang, and Nengqin Jia*

The Education Ministry Key Laboratory of Resource Chemistry and Shanghai Key Laboratory of Rare Earth Functional Materials, Department of Chemistry, College of Life and Environmental Sciences, Shanghai Normal University, 100 Guilin Road, Shanghai 200234, China

S *Supporting Information*

ABSTRACT: Fluorescence polarization (FP)-based signal is a self-referencing fluorescence signal, and it is less dependent on dye concentration and environmental interferences, which makes FP measurement an attractive alternative sensing technology to fluorescence intensity-based detection. However, most of the fluorescence polarization probes were constructed by introducing fluorescein, rhodamine, and cyanine dyes, which have relatively shorter excited-state lifetimes compared with BODIPY and naphthalimide dyes. Herein, a first naphthalimide based fluorescence polarization probe (**BIO**) was designed and synthesized for selective and direct detection of cancer cells. The relatively longer excited-state lifetimes and high photostability of naphthalimide makes **BIO** more sensitive and accuracy in quantitative determination of HeLa cells in homogeneous solution without cell lysis and further separation steps. The detection limit of **BIO** for HeLa cells was about 85 cells mL^{-1}, the linear range was from 2.5×10^2 cells mL^{-1} to 1×10^6 cells mL^{-1} and the response time is no more than 25 min. Moreover, due to the relatively high photostability of naphthalimide, **BIO** was particularly suitable for live cell imaging under continuous irradiation with confocal microscopy, and the specific interaction of **BIO** with CD44-overexpressing cell lines was clearly visualized. Importantly, this **BIO** based sensing platform offers a direct and real-time tool for cancer cell diagnosis when complemented with the use of naphthalimide-based fluorescence polarization probe.

KEYWORDS: *naphthalimide, fluorescence polarization probe, lifetime, cancer cells, self-referencing fluorescence sensing technology, live cell imaging*

INTRODUCTION

The past decades have witnessed significant advances in fluorescence based sensing technology including development of new fluorescence sensing mechanism and measurement instrumentation.[1,2] Fluorescence sensing technology has been viewed as a powerful and versatile toolbox in the field of physiology and molecular biology, environmental monitoring and clinical diagnosis with the advantage of high selectivity and sensitivity, spatiotemporal resolution, and visibility.[2−5] However, the fluorescence intensity based assay might be interfered with by some environmental factors such pH changes, fluorescence self-quenching, and large background signal. Thus, self-calibration should be required for improving the accuracy and reliability of the fluorescence sensing technology. Recently, two major self-referencing approaches including the fluorescence ratiometric method[6] and lifetime detection[7−10] were developed for overcoming the obstacles of fluorescence intensity based assay, which makes the detection sufficiently reliable. Despite these efforts, rapid, simple, and convenient self-referencing fluorescence detection techniques are still urgently needed especially for cancer diagnosis.[6,11−13]

Fluorescence polarization (FP) measurement is another self-referencing fluorescence sensing technology. Because the polarization value (P) is defined as the ratio of fluorescence intensities parallel ($I_{\parallel}$) and perpendicular ($I_{\perp}$) with respect to plane-polarized excitation light (eq 1, detailed information, please see ref 14), the fluorescence polarization-based signal is less dependent on dye concentration and environmental interference, which makes FP measurement an attractive alternative to fluorescence intensity-based detection.[15,16] Meanwhile, FP assay is a "mix and measure" technique without separation of the free and bound ligands, which make FP more convenient for real-time monitoring of the dynamic changes of biomacromolecules including membrane lipid mobility,[17−19] DNA−protein and protein−protein interactions,[20,21] and folding of G-quadruplex motif,[22] as well as the hyaluronidase activity[23] at the molecular level.[24−26] Apart from detection of biomacromolecules, recent years have also witnessed substantial progress in aptamer based fluorescence polarization measurement in determining small molecules such as Ochratoxin A,[27,28] ATP,[29−31] adenosine, and adenosine monophosphate,[32] as well as L-tyrosinamide.[33,34]

Table 1. Lifetime and Photostability of Naphthalimide-Based BIO Compared to Other Fluorescent Dyes

	fluorescein dyes	rhodamine dyes	cyanine dyes	BODIPY dyes	naphthalimide dyes	**BIO**
lifetime (ns)	4^a	$2-4^a$	1^a	6^b	$7-8^c$	6.26^d
photostability	low[e]	low[e]	low[b]	relatively high[f]	relatively high[e]	relatively high
used in fluorescence polarization assay	common	common	rare	common	rare	this work

[a]Refs 35,36. [b]Ref 37. [c]Ref 38. [d]Data was acquired by single-photon counting technique (detailed information in Supporting Information). [e]Ref 49. [f]Ref 52.
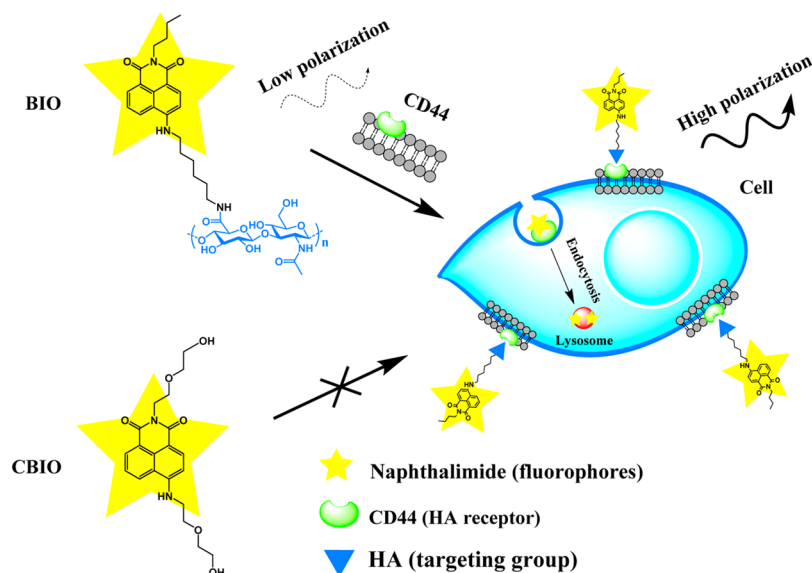

Figure 1. Illustration of fluorescence polarization probe **BIO** in the detection of CD44 in situ on cell membranes and intracellular transport CD44 via endocytosis.

$$P = \frac{I_\parallel - GI_\perp}{I_\parallel + GI_\perp} \qquad G = I_{HV}/I_{HH} \qquad (1)$$

However, most of these fluorescence polarization probes were constructed by introducing fluorescein (or its derivatives such as FAM, a commercially available dye), rhodamine, and cyanine dyes, which have relatively short excited-state lifetimes (less than 4 ns)[35,36] compared to BODIPY and naphthalimide dyes (lifetimes of naphthalimide and BODIPY dyes were above 6 ns, Table 1).[37,38] In addition, the longer excited-state lifetimes of BODIPY and naphthalimide dyes could make the signal of fluorescence polarization more sensitive to binding interactions over a larger molecular weight range.[37] Some BODIPY based fluorescence polarization probes have been used for detection of biological samples,[39−42] but the naphthalimide-based fluorescence polarization probes are still rarely investigated in the biological assay (Table 1). Furthermore, most fluorescence polarization probes for cancer diagnosis were mainly based on determination of concentration of biomarker in cancer cells. There are only a few fluorescence polarization probes developed for direct detection of cancer cells.[43−45] Due to the significant role of direct capture of cancer cells, especially in circulating tumor cell (CTC) detection, development of a sensitive and convenient approach for direct detection of cancer cells will contribute to the potential clinical utilization in early cancer diagnosis.[46,47] Herein, a first naphthalimide-based fluorescence polarization probe was designed and synthesized for sensitive and direct detection of cancer cells.

The working principle of this naphthalimide-based fluorescence polarization technology is illustrated in Figure 1. The cancer cell-target fluorescence polarization probe (**BIO**) was prepared from 4-amino-1,8-naphthalimide dye and chemically modified hyaluronic acid (HA). Considering the longer excited-state lifetimes and greater photostability of naphthalimide compared with fluorescein and rhodamine dyes,[38,48,49] the 4-amino-1,8-naphthalimide was introduced into **BIO** to emit the fluorescence polarization signal. At the same time, we have chosen HA as a specific ligand for direct targeting of cancer cells because HA serves as a key signaling molecule in regulating cancer metastasis through the interaction with CD44 (a HA receptor), and the overexpressed CD44 is closely related to cancerous angiogenesis and other types of tumor progression. Consequently, the increase in the fluorescence polarization signal of **BIO** will become remarkable only upon capturing the target cancer cells. Compared to other current technologies for detection of cancer cells, **BIO** contains the following advantages: (a) the fluorescence polarization signal from **BIO** is a self-referencing signal which could not be interfered with by environment factors; (b) the longer excited-state lifetimes and higher photostability of 4-amino-1,8-naphthalimide makes **BIO** more sensitive and accurate in detecting cancer cells; (c) the relatively high photostable naphthalimide makes **BIO** particularly suitable to live cell imaging under continuous irradiation with confocal microscopy; (d) to the best of our knowledge, **BIO** is a rarely reported fluorescence polarization probe for directly detecting cancer cells in homogeneous solution, which enables real-time monitoring of living cancer cells without cell lysis and further separation steps.
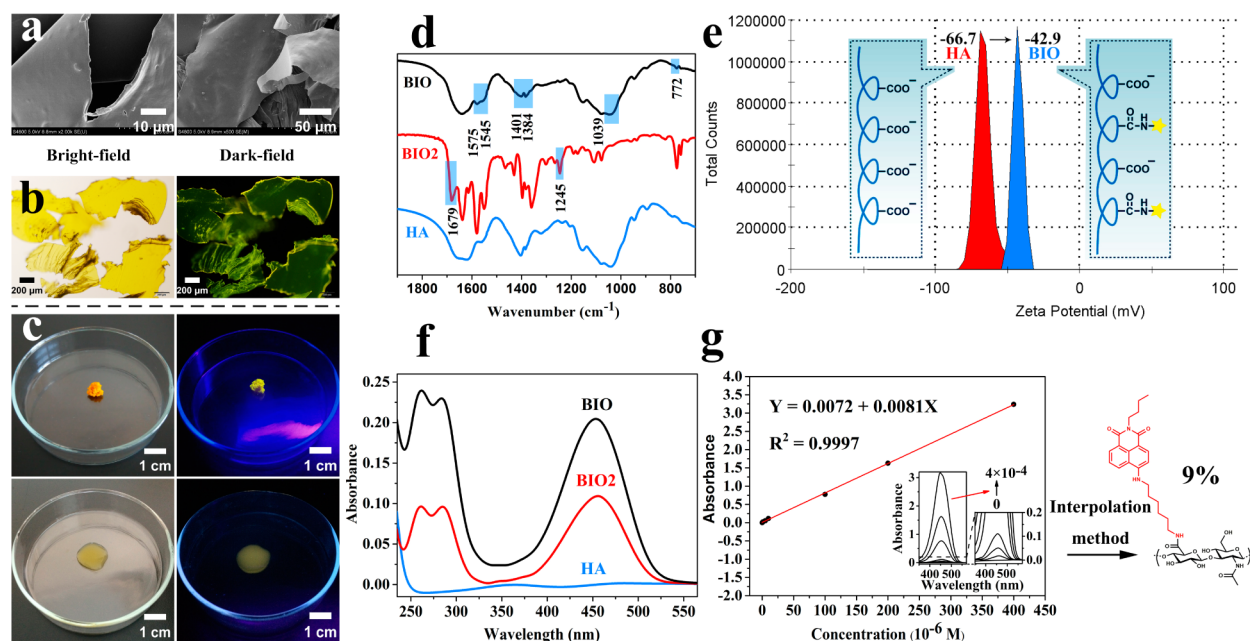
Figure 2. Series of characterizations of **BIO**. (a) SEM images of lamellar probe **BIO** after drying at a low temperature. (b) Microscopy images of **BIO** (left: bright field, right: fluorescence images under 405 nm exictation), scale bar, 200 μm. (c) Dry (shrinking) and swelling status of probe **BIO** under the naked eye (left: bright field, right: fluorescence images under the UV lamp). (d) FT-IR spectra of HA (blue) and **BIO2** (red) and probe **BIO** (black). (e) Zeta potential shift from unmodified HA (red) to **BIO2**-modified probe **BIO** (blue). (f) UV−vis absorption spectra of HA, **BIO2**, and probe **BIO**. (g) UV−vis absorption spectra of different concentrations ($(0-4) \times 10^{-4}$ M) **BIO2** at 450 nm. Inset: changes in UV−vis absorption spectra of different amounts of **BIO2**. (**BIO2**-modification efficiency of **BIO** reaches 9% by interpolation analysis upon **BIO2** UV−vis absorption standard line.)

RESULTS AND DISCUSSION

Synthesis and Characterization of BIO. Our investigation began with the preparation of target probe **BIO**. As displayed in Scheme S1, N-butyl-4-(6′-aminohexyl)amino-1,8-naphthalimide (**BIO2**) was initially prepared through a facile procedure.[50,51] Then **BIO** was prepared by conjugation of **BIO2** and HA through the amide bond. The chemical structures of **BIO** were characterized by IR (Figure 2d), zeta potential, and UV−vis spectra (Figure 2f). The peaks at 1545 and 1384 cm^{-1} can be attributed to the N−H and C−N bands in the amide bond of **BIO**, and the strength of the peak at 772 cm^{-1} of **BIO** decreased compared with that of **BIO2**, which was ascribed to the disappearance of the primary amine of **BIO2** through the formation of an amide bond. The peak at 1039 cm^{-1} is from the HA (Figure 2d). Similarly, the zeta potential of **BIO** was −42.9 mV which is relatively positive compared to that of HA (−66.7 mV, Figure 2e), because some of the carboxylic acids in HA were replaced by amine groups of **BIO2** through the formation of amide bonds. A maximum absorption at about 450 nm appeared in the UV−vis spectra of **BIO** also suggesting that **BIO2** was successfully conjugated to HA. Furthermore, through the interpolation analysis based on the UV−vis absorption standard line, we observed that the **BIO2** modification efficiency of **BIO** reaches 9%. All these results suggest that **BIO** was successfully synthesized. Meanwhile, the morphology of **BIO** was also investigated in both solid state and water solution. Transmission electron microscopy (TEM) images reveal a lamellar structure in the dry form (Figure 2a), which also emitted yellow fluorescence at 405 nm excitation under microscopy (Figure 2b). After **BIO** was added into water, it swelled and became water-soluble. The water solubility of **BIO** makes it suitable for further application in biological samples under physiological conditions. Meanwhile, DLS (dynamic light scattering) analysis of **BIO** in water solution suggested that the hydrodynamic diameter of **BIO** was centered at 634.8 nm (Figure S2), and no other peak was observed in DLS analysis, indicating a pure **BIO** in water solution.

Fluorescence Lifetime of BIO and Cell Viability. Then, by using the single-photon counting technique (Edinburgh FL 900, detailed procedure in Supporting Information), the fluorescence lifetime of **BIO** was determined to be 6.26 ns (Table 1). Compared with fluorescein, rhodamine, and cyanine dyes, the naphthalimide-modified **BIO** displayed a relatively longer lifetime, which was beneficial for sensitive detection of HeLa cells through changes of the fluorescence polarization signal.

The cell cytotoxicity of **BIO** was also tested by MTT using a standard methyl thiazolyl tetrazolium (MTT) assay. During the concentration between 0 and 150 μg mL^{-1}, **BIO** exhibited no cell cytotoxicity (Figure S3) when the incubation time was 12 h. Even as the incubation time extends to 24 h, there was no obviously decrease in cell viability (Figure S3). All these results suggested that **BIO** could be used in the biological samples, especially for the detection of live cells.

Fluorescence Polarization Response of BIO to HeLa Cells. Next, we investigated the fluorescence polarization sensing behavior of **BIO** toward HeLa cells. Initially, pH titration was conducted in water. As shown in Figure S1, no significant difference in fluorescence of **BIO** was observed over the pH range of 6.5−10. Thus, a PBS buffer (pH 7.4, containing 1% DMSO) was chosen as the test medium. Then, we tested the effect of **BIO** concentration on the fluorescence polarization assay. As indicated in Figure 3a, 14.56 μg mL^{-1} of **BIO** was conducive to fluorescence polarization assay. If the concentration of **BIO** was higher or lower, the sensitivity of the fluorescence polarization signal would be decreased. Thus,
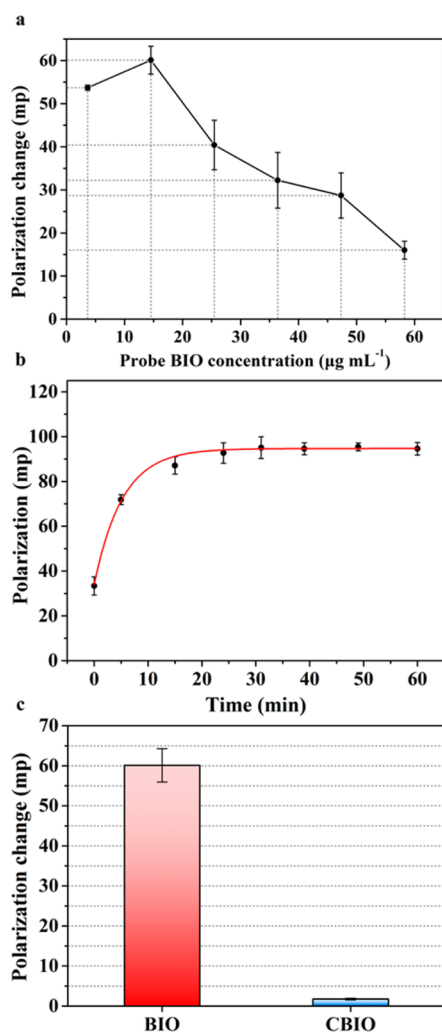
Figure 3. (a) Concentration effect of fluorescence polarization probe **BIO** on the polarization assay. The amount of detected target HeLa cells is 10^5 cells mL^{-1}. (b) Time correlation dynamics curve of fluorescence polarization probe **BIO** (14.56 μg mL^{-1}) for HeLa cells (10^5 cells mL^{-1}). (c) Fluorescence polarization response of **BIO** and control probe **CBIO** for HeLa cells (10^5 cells mL^{-1}).

14.56 μg mL^{-1} of **BIO** was used in the following assay. To obtain the optimal incubation time of interaction between **BIO** and HeLa cells, the dynamic changes of the fluorescence polarization signal of **BIO** were recorded through continuous observation. As displayed in Figure 3b, after 10^5 cells mL^{-1} of HeLa cells were added into PBS buffer containing 14.56 μg mL^{-1} of **BIO**, the fluorescence polarization signal changed quickly within 15 min and then reached a plateau after 25 min. This result demonstrated that the interaction between HeLa cells and **BIO** was nearly complete within 25 min. Therefore, 30 min was taken for the detection time in the following experiments.

To test whether **BIO** could be used in the specific recognition of HeLa cells, a control probe (**CBIO**) without the specific HA ligand was also synthesized for detection of HeLa cells (Figure 1, detailed synthetic procedures in Scheme S1). As shown in Figure 4c and Figure S4, negligible changes in the fluorescence polarization signal were observed when **CBIO** was incubated with HeLa cells. By contrast, the incubation between HeLa cells with **BIO** resulted in a remarkable increase in the fluorescence polarization signal, which could be ascribed to the specific binding of HA in **BIO** to the CD44 expressed on the HeLa cell surface. The rotation of **BIO** might become slow after **BIO** was bound to the CD44 on cell surface, which could result in an enhancement in fluorescence polarization signal. These results also demosntrated the high selectivity of **BIO** for determination of CD44-overexpressing cell lines.

Quantitative Determination of HeLa Cells with BIO. Then, **BIO** was used to determine the quantity of HeLa cells through the direct fluorescence polarization signal readout. As displayed in Figure 4a, the changes in fluorescence polarization signal increased upon gradual addition of increased concetration of HeLa cells (from 0 to 1×10^6 cells mL^{-1}). Through the enlarged profile (Figure 4a, inset), a clear and quick enhancement in fluorescence polarization signal could be obtained even when the concentration of HeLa cells fell below 2.5×10^2 cells mL^{-1}. Meanwhile, when the amount of HeLa cells increased to 1×10^6 cells mL^{-1}, the increase in fluorescence polarization signal beccame very slow. From the concentration-dependent fluorescence polarization changes, the limit of detection (LOD) of **BIO** for HeLa cells was about 85 cells mL^{-1} (S/N = 3). Additionally, we take the logarithm of fluorescence polarization changes and concentration of HeLa
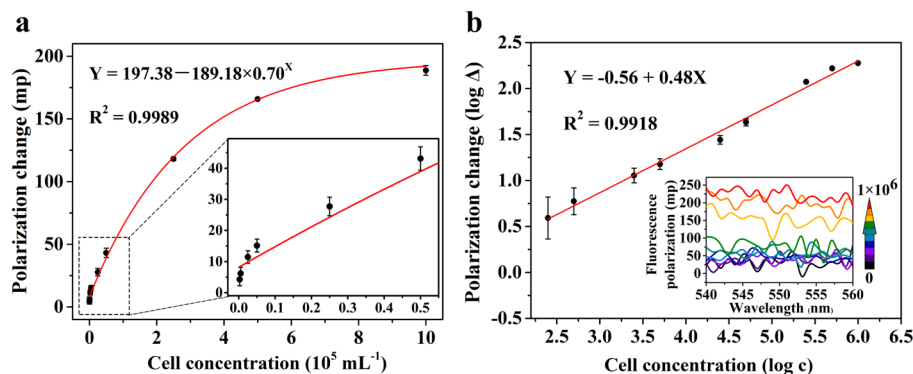

Figure 4. Quantitative analysis of the HeLa cells using fluorescence polarization assay based on **BIO** (14.56 μg mL^{-1}). (a) Fluorescence polarization response of **BIO** to different concentration of HeLa cells (($0-1) \times 10^6$ cells mL^{-1}). Inset: Enlarged profile of fluorescence polarization changes depending on low concentration of HeLa cells (($0-5) \times 10^4$ cells mL^{-1}). (b) Logarithmic behavior of fluorescence polarization changes with different concentration of HeLa cells. Inset: fluorescence polarization response of **BIO** for different amounts of HeLa cells (($0-1) \times 10^6$ cells mL^{-1}). Error bar represents s.d.

Table 2. Comparisons of the Proposed Fluorescence Polarization Probe BIO with Other Reported Sensors for HeLa Cell Detection

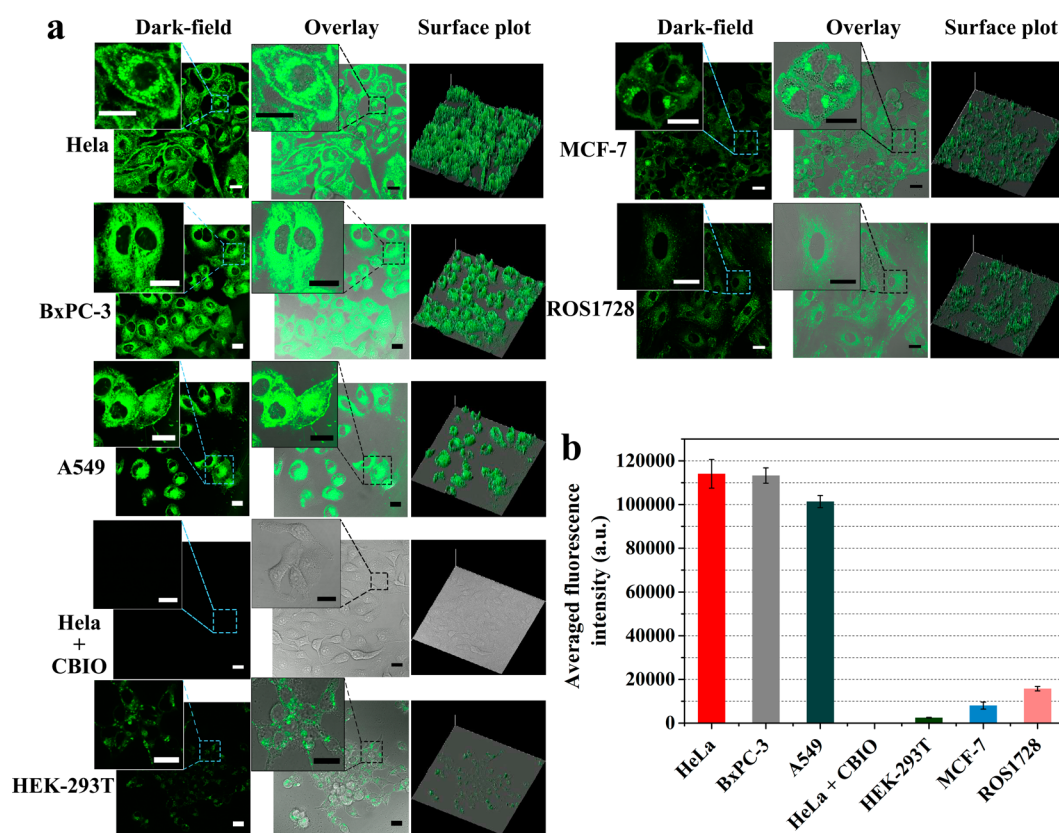| detection technique	materials for construction of probes (or sensors)	detection limit (cell mL^{-1})	linear range (cell mL^{-1})	type of cancer cells	references
chemiluminescence	G-quadruplex aptamers	6000	2×10^3–6×10^5	HeLa cells	Li et al. 2009[53]
electrochemical (impedance)	grapheme based aptasensor	794	1×10^3–1×10^6	HeLa cells	Feng et al. 2011[54]
electrochemical (AC impedimetric approach)	gold nanoparticles deposited on boron-doped diamond electrode	10	1×10^1–1×10^5	HeLa cells	Weng et al. 2011[55]
electrochemical (DPV)	PEI modified single-wall carbon nanotubes	10	1×10^1–1×10^6	HeLa cells	Liu et al. 2013[56]
electrochemical (impedance)	folate conjugated PEI modified carbon nanotubes	90	2.4×10^2–2.4×10^5	HeLa cells	Wang et al. 2013[57]
fluorescence polarization	naphthalimide modified HA	85	2.5×10^2–1×10^6	HeLa cells	This work

Figure 5. Live cell imaging on six types of cell lines with CD44 expression in different levels with **BIO** and control probe **CBIO**. (a) Confocal microscopy images (dark-field and overlay) of CD44-overexpressing cell lines (HeLa cells, BxPC-3 cells, and A549 cells) and cell lines with low expression of CD44 (MCF-7 cells, ROS1728 cells (rat osteosarcoma cell line), and HEK-293T cells) incubated with probe **BIO**, and HeLa cells incubated with control probe **CBIO** for 30 min at 37 °C. (b) Histogram showing the semiquantitative calculation of averaged fluorescence intensity (FI) of each cell in the displayed images. Scale bars are 20 μm.

cells, which was defined as (log(Δ) and log(c)), respectively. With a linear regression by *Origin 8.0* software, a linear relationship between (log(Δ) and log(c)) was observed (Figure 4b, R^2 = 0.9918). Therefore, a linear relationship between changes of fluorescence polarization signal and the concentrations of HeLa cells (changes from 2.5×10^2 cells mL^{-1} to 1×10^6 cells mL^{-1}, Figure 4b) can be deduced. The obtained linear curve makes quantitative detection of HeLa cells very convenient over this concentration range. Compared to some of the other cytosensors for cancer cells, the probe **BIO** exhibited a relatively lower detection limit and wider linear range (Table 2, Table S1).[53−62] Moreover, most cytosensors were developed based on electrochemical approaches, and the

fluorescence polarization probe **BIO** could be an alternative to these electrochemical approaches for detection of cancer cells (Table 2, Table S1). Finally, **BIO** also presents a platform for quantitative determination of other CD44-overexpressing cancer cells by using fluorescence polarization detection.

Live Cell Imaging with BIO. To further investigate whether **BIO** could be used as a fluorescent tool for visualized monitoring of CD44-overexpressing cancer cells, live-cell imaging exepriments in CD44-overexpressing cell lines (including HeLa cells, BxPC-3 cells and A549 cells) and cell lines with low-level expression of HA (including ROS1728 (rat osteosarcoma cell line), MCF-7 cells (human breast cancer cell line) and HEK-293T cells) with **BIO** were conducted,
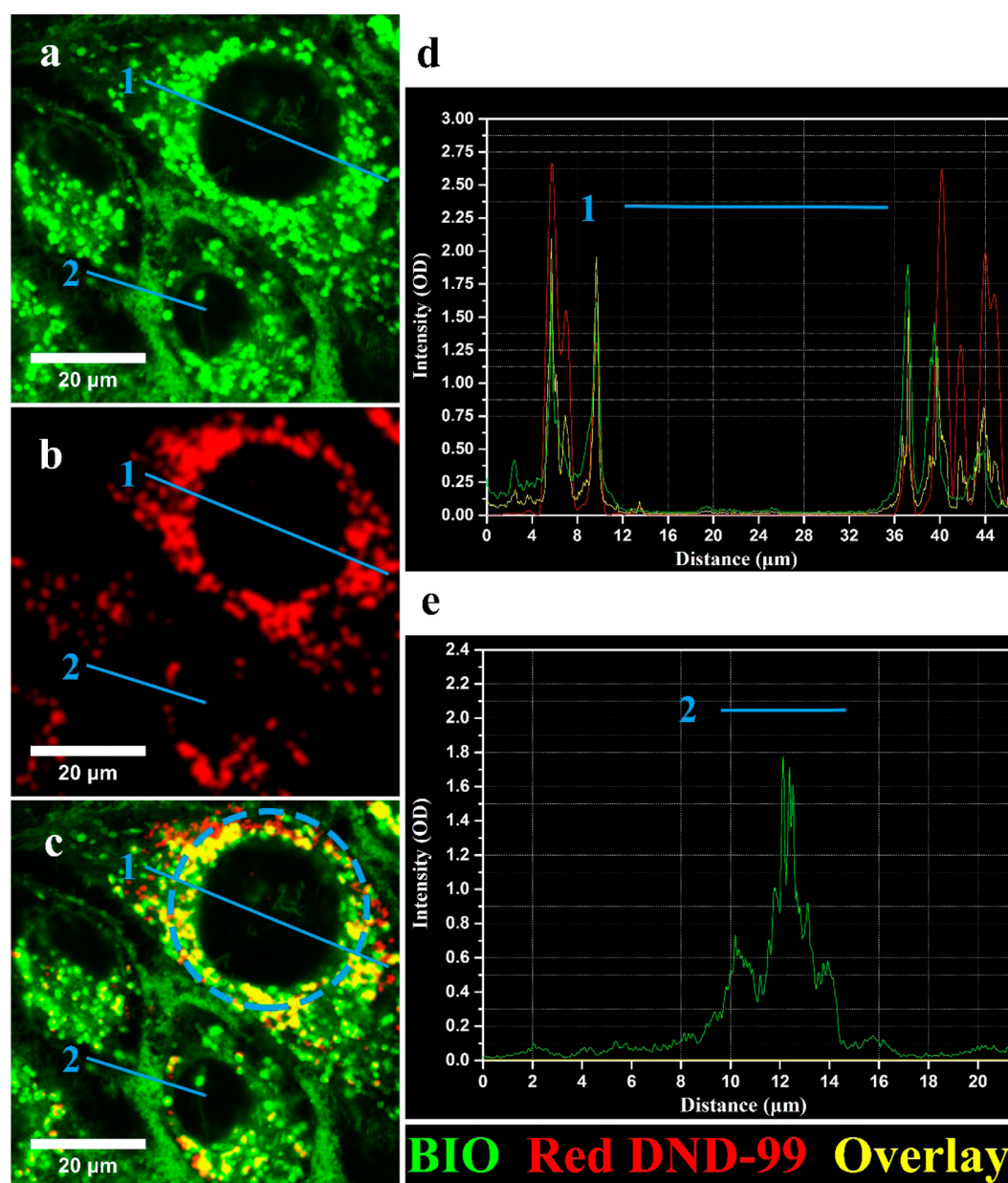
Figure 6. Fluorescent image of target HeLa cells co-stained with **BIO** and commercial lysosome-probe Red DND-99. (a) Confocal microscopy image of HeLa cells incubated with **BIO** (14.56 μg mL^{-1}) (λ_{ex} = 458 nm, λ_{em} = 510−590 nm, green). (b) Confocal microscopy image of HeLa cells stained with Red DND-99 (50 nM) (λ_{ex} = 633 nm, λ_{em} = 640−795 nm, red). (c) Overlay image of (a) and (b) (Pearson's correlation R_r = 0.815 and overlap coefficient R = 0.835 of lysosome colocalization in dashed circular area). (d) Intensity profile of regions of interest (ROI) (1, lysosome-location) across HeLa cells. (e) Intensity profile of regions of interest (ROI) (2, cell-membrane-location) across HeLa cells. Scale bars are 20 μm.

respectively. As suggested in Figure 5a, after the cells were incubated with **BIO** for 30 min at 37 °C, a strong fluorescence signal was obtained in HeLa cells, BxPC-3 cells, and A549 cells upon 458 nm excitation with the confocal microscopy, while the **BIO**-treated ROS1728, MCF-7, and HEK-293T cells produced a relatively weak fluorescence signal. Meanwhile, treatment of HeLa cells with the control probe **CBIO** only leads to a negligible fluorescence signal. Additionally, through the semiquantitative calculation of averaged emission intensity in cells (Figure 5b), we can see clearly that there was an approximately 6-fold enhancement in fluorescence intensity of **BIO**-treated HeLa, BxPC-3, and A549 cells compared to **BIO**-treated ROS1728, MCF-7, and HEK-293T cells. This result demonstrated that HeLa cells, BxPC-3 cells, and A549 cells

contain a high level of CD44, and there was low-level expression of ROS1728, MCF-7, and HEK-293T cells, which was partially supported by a previous study that reveals an overexprssion of CD44 on HeLa cells, BxPC-3 cells, and A549 cells and low-level expression of CD44 in ROS1728 cells, MCF-7 cells, and HEK-293T cells.[63−65] It is interesting that this result also indentified that ROS1728 cells expressed only a little amount of CD44. There is little study revealing the expressed amount of CD44 on ROS1728, which might be potentially useful for understanding bone remodeling.[66] For the **CBIO** treated HeLa cells, the semiquantitative calculation of averaged emission intensity only emits a background signal, which indicated that specific binding of **BIO** to HeLa cells occurred through the specific interaction between HA of **BIO**

and CD44 on live cells. All these results indicated that **BIO** was a highly selective probe for determining CD44-overexpressing HeLa cells, and this fluorecence polarization technique with **BIO** could be potentially used for detecting other CD44-overexpressing cancer cells.

Subcellular Distribution Study of BIO on HeLa Cells. Encouraged by the specific interaction of **BIO** with CD44-overexpressing HeLa cells, the subcellular distribution of **BIO** on HeLa cells was finally investigated. As displayed in Figure 5a and Figure S5, a strong fluorescence signal mainly concentrated in the cell membrane and dot-like vesicular in cytoplasm was observed, suggesting a membrane and lysosomal localization. Then, a colocalization experiment was performed by co-staining HeLa cells with LysoTracker Red DND-99 (a commercially available probe for specific staining of lysosomes). Through the fluorescence signal obtained under confocal microscopy, the subcellular localization of **BIO** could be visualized. As illustrated in Figure 6, a strong green fluorescecne signal was from **BIO**, and the red fluorescence signal was attributed to the localization of LysoTracker Red DND-99 stained lysosomes. The merged images of **BIO** and LysoTracker Red DND-99 stained signal showed the strong yellow fluorescence, which mainly localized in lysosomes (Figure 6a,b,c). Through the plot analysis of regions interest (ROI) across the HeLa cells (line 1 in Figure 6a,b,cd), we can observe that some of the **BIO** stained singal and LysoTracker Red DND-99 stained lysosomes overlapped well. This result depicted that some **BIO** was localized in lysosomes. Additionally, plot analysis of ROI also suggested a strong green fluorescence signal on cell membrane (line 2 in Figure 6a,b,c,e). Thus, the high selectivity of **BIO** for HeLa cells was mainly based on the specific interaction of HA of **BIO** with CD44 on HeLa cell membranes. Then, some **BIO** penetrated into HeLa cells through a CD44-mediated endocytosis and finally localized in lysosomes.[63,67,68]

■ CONCLUSION

In summary, a naphthalimide-based fluorescence polarization probe (**BIO**) was designed and synthesized for selective and direct detection of CD44-overexpressing HeLa cells. To the best of our knowledge, **BIO** was the first naphthalimide-modified HA based fluorescence polarization probe for detection of cancer cells. Compared to previous fluorescein (or rhodamine)-modified HA based fluorescence polarization probe, **BIO** with the naphthalimide fluorophore embodies the relatively high photostability and longer lifetime. Through the direct readout of changes in fluorescence polarization signal of **BIO**, we have described a new approach for detection of CD44-overexpressing HeLa cells in no more than 25 min. Importantly, this fluorescence polarization technique permits an accurate and quantative determination of HeLa cells through the self-referencing fluorescence polarization signal. This fluorescence polarization based technique for direct detection of cancer cells also presents potential utilization in CTC detection. Finally, the subcellular distribution of **BIO** on HeLa cells was investigated through the confocal microscopy assay, which could further indentify the high selectivity of **BIO** for cancer cells with overexpressed CD44. On the basis of **BIO**, a direct and real-time tool has been developed for detecting cancer cells in homogeneous solution, which enables monitoring of living cancer cells without cell lysis and further separation steps and could offer more accurate information for cancer clinical diagnosis.

■ ASSOCIATED CONTENT

⑤ Supporting Information
Additional materials and methods. The Supporting Information is available free of charge on the ACS Publications website at DOI: 10.1021/acsami.5b02429.

■ AUTHOR INFORMATION

Corresponding Authors
*E-mail: huangcs@shnu.edu.cn.
*E-mail: nqjia@shnu.edu.cn.

Notes
The authors declare no competing financial interest.

■ ABBREVIATIONS

FP, fluorescence polarization; HA, hyaluronic acid

■ REFERENCES

(1) Lakowicz, J. R. In *Topics in Fluorescence Spectroscopy*; Lakowicz, J. R., Valeur, B., Czarnik, A. W., Eds.; Springer, 1991; Vol. 4, pp 1−68.

(2) de Silva, A. P.; Gunaratne, H. Q. N.; Gunnlaugsson, T.; Huxley, A. J. M.; McCoy, C. P.; Rademacher, J. T.; Rice, T. E. Signaling Recognition Events with Fluorescent Sensors and Switches. *Chem. Rev.* **1997**, *97*, 1515−1566.

(3) Chan, J.; Dodani, S. C.; Chang, C. J. Reaction-based Small-Molecule Fluorescent Probes for Chemoselective Bioimaging. *Nat. Chem.* **2012**, *4*, 973−984.

(4) Stennett, E. M. S.; Ciuba, M. A.; Levitus, M. Photophysical Processes in Single Molecule Organic Fluorescent Probes. *Chem. Soc. Rev.* **2014**, *43*, 1057−1075.

(5) Li, H.; Fan, J.; Peng, X. Colourimetric and Fluorescent Probes for the Optical Detection of Palladium Ions. *Chem. Soc. Rev.* **2013**, *42*, 7943−7962.

(6) Fan, J.; Hu, M.; Zhan, P.; Peng, X. Energy Transfer Cassettes Based on Organic Fluorophores: Construction and Applications in Ratiometric Sensing. *Chem. Soc. Rev.* **2013**, *42*, 29−43.

(7) Levitt, J. A.; Kuimova, M. K.; Yahioglu, G.; Chung, P.-H.; Suhling, K.; Phillips, D. Membrane-Bound Molecular Rotors Measure Viscosity in Live Cells via Fluorescence Lifetime Imaging. *J. Phys. Chem. C* **2009**, *113*, 11634−11642.

(8) Nie, S.; Zare, R. N. Optical Detection of Single Molecules. *Annu. Rev. Biophys. Biomol. Struct.* **1997**, *26*, 567−596.

(9) Barker, S. L. R.; Clark, H. A.; Swallen, S. F.; Kopelman, R.; Tsang, A. W.; Swanson, J. A. Ratiometric and Fluorescence-Lifetime-Based Biosensors Incorporating Cytochrome c and the Detection of Extra- and Intracellular Macrophage Nitric Oxide. *Anal. Chem.* **1999**, *71*, 1767−1772.

(10) Kuimova, M. K.; Yahioglu, G.; Levitt, J. A.; Suhling, K. Molecular Rotor Measures Viscosity of Live Cells via Fluorescence Lifetime Imaging. *J. Am. Chem. Soc.* **2008**, *130*, 6672−6673.

(11) Kucherak, O. A.; Oncul, S.; Darwich, Z.; Yushchenko, D. A.; Arntz, Y.; Didier, P.; Mély, Y.; Klymchenko, A. S. Switchable Nile Red-Based Probe for Cholesterol and Lipid Order at the Outer Leaflet of Biomembranes. *J. Am. Chem. Soc.* **2010**, *132*, 4907−4916.

(12) Rossignol, R.; Gilkerson, R.; Aggeler, R.; Yamagata, K.; Remington, S. J.; Capaldi, R. A. Energy Substrate Modulates Mitochondrial Structure and Oxidative Capacity in Cancer Cells. *Cancer Res.* **2004**, *64*, 985−993.

(13) Shynkar, V. V.; Klymchenko, A. S.; Kunzelmann, C.; Duportail, G.; Muller, C. D.; Demchenko, A. P.; Freyssinet, J.-M.; Mely, Y. Fluorescent Biomembrane Probe for Ratiometric Detection of Apoptosis. *J. Am. Chem. Soc.* **2007**, *129*, 2187−2193.

(14) Johnson, I.; Spence, M. *The Molecular Probes Handbook: A Guide to Fluorescent Probes and Labeling Technologies*, 11th ed; Life Technologies Corporation, 2010; Chapter 1, pp 44−46.

(15) Jameson, D. M.; Ross, J. A. Fluorescence Polarization/ Anisotropy in Diagnostics and Imaging. *Chem. Rev.* **2010**, *110*, 2685−2708.

(16) Checovich, W. J.; Bolger, R. E.; Burke, T. Fluorescence Polarization -A New Tool for Cell and Molecular Biology. *Nature* **1995**, *375*, 254−256.

(17) Fuchs, P.; Parola, A.; Robbins, P. W.; Blout, E. R. Fluorescence Polarization and Viscosities of Membrane Lipids of 3T3 Cells. *Proc. Natl. Acad. Sci.* **1975**, *72*, 3351−3354.

(18) Martin, C. E.; Thompson, G. A. Use of Fluorescence Polarization to Monitor Intracellular Membrane Changes During Temperature Acclimation. Correlation with Lipid Compositional and Ultrastructural Changes. *Biochemistry* **1978**, *17*, 3581−3586.

(19) Schachter, D.; Shinitzky, M. Fluorescence Polarization Studies of Rat Intestinal Microvillus Membranes. *J. Clin. Invest.* **1977**, *59*, 536−548.

(20) Jameson, D. M.; Seifried, S. E. Quantification of Protein−Protein Interactions Using Fluorescence Polarization. *Methods* **1999**, *19*, 222−233.

(21) Lundblad, J. R.; Laurance, M.; Goodman, R. H. Fluorescence Polarization Analysis of Protein-DNA and Protein-Protein Interactions. *Mol. Endocrinol.* **1996**, *10*, 607−612.

(22) Zhang, D.; Shen, H.; Li, G.; Zhao, B.; Yu, A.; Zhao, Q.; Wang, H. Specific and Sensitive Fluorescence Anisotropy Sensing of Guanine-Quadruplex Structures via a Photoinduced Electron Transfer Mechanism. *Anal. Chem.* **2012**, *84*, 8088−8094.

(23) Murai, T.; Kawashima, H. A Simple Assay for Hyaluronidase Activity Using Fluorescence Polarization. *Biochem. Biophys. Res. Commun.* **2008**, *376*, 620−624.

(24) Borenstain, V.; Barenholz, Y. Characterization of Liposomes and Other Lipid Assemblies by Multiprobe Fluorescence Polarization. *Chem. Phys. Lipids* **1993**, *64*, 117−127.

(25) Bachovchin, D. A.; Brown, S. J.; Rosen, H.; Cravatt, B. F. Identification of Selective Inhibitors of Uncharacterized Enzymes by High-Throughput Screening with Fluorescent Activity-Based Probes. *Nat. Biotechnol.* **2009**, *27*, 387−394.

(26) Heyduk, T.; Ma, Y.; Tang, H.; Ebright, R. H. Fluorescence Anisotropy: Rapid, Quantitative Assay for Protein-DNA and Protein-Protein Interaction. In *Methods in Enzymology*, Sankar, A., Ed.; Academic Press, 1996; pp 492−503.

(27) Cruz-Aguado, J. A.; Penner, G. Fluorescence Polarization Based Displacement Assay for the Determination of Small Molecules with Aptamers. *Anal. Chem.* **2008**, *80*, 8853−8855.

(28) Zhao, Q.; Lv, Q.; Wang, H. Identification of Allosteric Nucleotide Sites of Tetramethylrhodamine-Labeled Aptamer for Noncompetitive Aptamer-Based Fluorescence Anisotropy Detection of a Small Molecule, Ochratoxin A. *Anal. Chem.* **2013**, *86*, 1238−1245.

(29) Cui, L.; Zou, Y.; Lin, N.; Zhu, Z.; Jenkins, G.; Yang, C. J. Mass Amplifying Probe for Sensitive Fluorescence Anisotropy Detection of Small Molecules in Complex Biological Samples. *Anal. Chem.* **2012**, *84*, 5535−5541.

(30) Liu, J.; Wang, C.; Jiang, Y.; Hu, Y.; Li, J.; Yang, S.; Li, Y.; Yang, R.; Tan, W.; Huang, C. Graphene Signal Amplification for Sensitive and Real-Time Fluorescence Anisotropy Detection of Small Molecules. *Anal. Chem.* **2013**, *85*, 1424−1430.

(31) Huang, Y.; Zhao, S.; Chen, Z.; Shi, M.; Liang, H. Amplified Fluorescence Polarization Aptasensors Based on Structure-Switching-Triggered Nanoparticles Enhancement for Bioassays. *Chem. Commun.* **2012**, *48*, 7480−7482.

(32) Perrier, S.; Ravelet, C.; Guieu, V.; Fize, J.; Roy, B.; Perigaud, C.; Peyrin, E. Rationally Designed Aptamer-Based Fluorescence Polar-

ization Sensor Dedicated to the Small Target Analysis. *Biosens. Bioelectron.* **2010**, *25*, 1652−1657.

(33) Ruta, J.; Perrier, S.; Ravelet, C.; Fize, J.; Peyrin, E. Noncompetitive Fluorescence Polarization Aptamer-Based Assay for Small Molecule Detection. *Anal. Chem.* **2009**, *81*, 7468−7473.

(34) Zhu, Z.; Schmidt, T.; Mahrous, M.; Guieu, V.; Perrier, S.; Ravelet, C.; Peyrin, E. Optimization of the Structure-Switching Aptamer-Based Fluorescence Polarization Assay for the Sensitive Tyrosinamide Sensing. *Anal. Chim. Acta* **2011**, *707*, 191−196.

(35) Nau, W. M.; Mohanty, J. Taming Fluorescent Dyes with Cucurbituril. *Int. J. Photoenergy* **2005**, *7*, 133−141.

(36) Marquez, C.; Nau, W. M. Polarizabilities Inside Molecular Containers. *Angew. Chem., Int. Ed.* **2001**, *40*, 4387−4390.

(37) Johnson, I, Spence, M. T. Z. *Molecular Probes Handbook: A Guide to Fluorescent Probes and Labeling Technologies*, 11th ed.; Invitrogen Life Technologies: Carlsbad, CA, USA, 2010.

(38) Ren, J.; Zhao, X.; Wang, Q.; Ku, C.; Qu, D.; Chang, C.; Tian, H. Synthesis and Fluorescence Properties of Novel Co-facial Folded Naphthalimide Dimers. *Dyes Pigments* **2005**, *64*, 179−186.

(39) Zhao, G.; Meier, T. I.; Kahl, S. D.; Gee, K. R.; Blaszczak, L. C. BOCILLIN FL, a Sensitive and Commercially Available Reagent for Detection of Penicillin-Binding Proteins. *Antimicrob. Agents Chemother.* **1999**, *43*, 1124−1128.

(40) Banks, P.; Harvey, M. Considerations for Using Fluorescence Polarization in the Screening of G Protein-Coupled Receptors. *J. Biomol. Screening* **2002**, *7*, 111−117.

(41) Banks, P.; Gosselin, M.; Prystay, L. Impact of a Red-Shifted Dye Label for High Throughput Fluorescence Polarization Assays of G Protein-Coupled Receptors. *J. Biomol. Screening* **2000**, *5*, 329−334.

(42) Schade, S. Z.; Jolley, M. E.; Sarauer, B. J.; Simonson, L. G. BODIPY−α-Casein, a pH-Independent Protein Substrate for Protease Assays Using Fluorescence Polarization. *Anal. Biochem.* **1996**, *243*, 1−7.

(43) Deng, T.; Li, J.; Zhang, L.; Jiang, J.; Chen, J.; Shen, G.; Yu, R. A Sensitive Fluorescence Anisotropy Method for the Direct Detection of Cancer Cells in Whole Blood Based on Aptamer-Conjugated Near-Infrared Fluorescent Nanoparticles. *Biosens. Bioelectron.* **2010**, *25*, 1587−1591.

(44) Tsuda, H.; Maeda, H.; Kishimoto, S. Fluorescence Polarization with FDA in Leukaemic Cells: A Clear Difference Between Myelogenous and Lymphocytic Origins. *Br. J. Cancer* **1981**, *43*, 793−803.

(45) Kornilova, A. Y.; Algayer, B.; Breslin, M.; Addona, G. H.; Uebele, V. Development of A Fluorescence Polarization Binding Assay for Folate Receptor. *Anal. Biochem.* **2013**, *432*, 59−62.

(46) Cristofanilli, M.; Budd, G. T.; Ellis, M. J.; Stopeck, A.; Matera, J.; Miller, M. C.; Reuben, J. M.; Doyle, G. V.; Allard, W. J.; Terstappen, L. W. M. M.; Hayes, D. F. Circulating Tumor Cells, Disease Progression, and Survival in Metastatic Breast Cancer. *New Engl. J. Med.* **2004**, *351*, 781−791.

(47) Paterlini-Brechot, P.; Benali, N. L. Circulating Tumor Cells (CTC) Detection: Clinical Impact and Future Directions. *Cancer Lett.* **2007**, *253*, 180−204.

(48) Wang, Q.; Ren, J.; Qu, D.; Zhao, X.; Chen, K.; Tian, H.; Erk, P. Synthesis and Luminescent Properties of Some Novel Naphthalimide Dimers. *Dyes Pigments* **2003**, *59*, 143−152.

(49) Huang, C.; Yin, Q.; Zhu, W.; Yang, Y.; Wang, X.; Qian, X.; Xu, Y. Highly Selective Fluorescent Probe for Vicinal-Dithiol-Containing Proteins and In Situ Imaging in Living Cells. *Angew. Chem., Int. Ed.* **2011**, *50*, 7551−6.

(50) Huang, C.; Li, H.; Luo, Y.; Xu, L. A Naphthalimide-Based Bifunctional Fluorescent Probe for the Differential Detection of Hg^{2+} and Cu^{2+} in Aqueous Solution. *Dalton Trans.* **2014**, *43*, 8102−8108.

(51) Un, H.; Wu, S.; Huang, C.; Xu, Z.; Xu, L. A Naphthalimide-Based Fluorescent Probe for Highly Selective Detection of Histidine in Aqueous Solution and Its Application in In Vivo Imaging. *Chem. Commun.* **2015**, *51*, 3143−3146.

(52) Hinkeldey, B.; Schmitt, A.; Jung, G. Comparative Photostability Studies of BODIPY and Fluorescein Dyes by Using Fluorescence Correlation Spectroscopy. *ChemPhysChem* **2008**, *9*, 2019−2027.

(53) Li, T.; Shi, L.; Wang, E.; Dong, S. Multifunctional G-Quadruplex Aptamers and Their Application to Protein Detection. *Chem.—Eur. J.* **2009**, *15*, 1036−1042.

(54) Feng, L.; Chen, Y.; Ren, J.; Qu, X. A Graphene Functionalized Electrochemical Aptasensor for Selective Label-Free Detection of Cancer Cells. *Biomaterials* **2011**, *32*, 2930−2937.

(55) Weng, J.; Zhang, Z.; Sun, L.; Wang, J. A. High Sensitive Detection of Cancer Cell with A Folic Acid-Based Boron-Doped Diamond Electrode Using an AC Impedimetric Approach. *Biosens. Bioelectron.* **2011**, *26*, 1847−1852.

(56) Liu, J.; Qin, Y.; Li, D.; Wang, T.; Liu, Y.; Wang, J.; Wang, E. Highly Sensitive and Selective Detection of Cancer Cell with A Label-Free Electrochemical Cytosensor. *Biosens. Bioelectron.* **2013**, *41*, 436−441.

(57) Wang, Z.; Chen, S.; Hu, C.; Cui, D.; Jia, N. An Enhanced Impedance Cytosensor Based on Folate Conjugated-Polyethyleni-mine-Carbon Nanotubes for Tumor Targeting. *Electrochem. Commun.* **2013**, *29*, 4−7.

(58) Qian, Z.; Bai, H.; Wang, G.; Xu, J.; Chen, H. A Photo-electrochemical Sensor Based on CdS-Polyamidoamine Nano-Composite Film for Cell Capture and Detection. *Biosens. Bioelectron.* **2010**, *25*, 2045−2050.

(59) Yang, G.; Cao, J.; Li, L.; Rana, R. K.; Zhu, J.-J. Carboxymethyl Chitosan-Functionalized Graphene for Label-Free Electrochemical Cytosensing. *Carbon* **2013**, *51*, 124−133.

(60) Gu, M.; Zhang, J.; Li, Y.; Jiang, L.; Zhu, J. Fabrication of A Novel Impedance Cell Sensor Based on the Polystyrene/Polyaniline/ Au Nanocomposite. *Talanta* **2009**, *80*, 246−249.

(61) Li, T.; Fan, Q.; Liu, T.; Zhu, X.; Zhao, J.; Li, G. Detection of Breast Cancer Cells Specially and Accurately by An Electrochemical Method. *Biosens. Bioelectron.* **2010**, *25*, 2686−2689.

(62) Hao, C.; Yan, F.; Ding, L.; Xue, Y.; Ju, H. A Self-Assembled Monolayer Based Electrochemical Immunosensor for Detection of Leukemia K562A Cells. *Electrochem. Commun.* **2007**, *9*, 1359−1364.

(63) Tran, T. H.; Choi, J. Y.; Ramasamy, T.; Truong, D. H.; Nguyen, C. N.; Choi, H.-G.; Yong, C. S.; Kim, J. O. Hyaluronic Acid-Coated Solid Lipid Nanoparticles for Targeted Delivery of Vorinostat to CD44 Overexpressing Cancer Cells. *Carbohyd. Polym.* **2014**, *114*, 407−415.

(64) Harada, H.; Nakata, T.; Hirota-takahata, Y.; Tanaka, I.; Nakajima, M.; Takahashi, M. F-16438s, Novel Binding Inhibitors of CD44 and Hyaluronic Acid. *J. Antibiot.* **2006**, *59*, 770−776.

(65) Takada, M.; Yamamoto, M.; Saitoh, Y. The Significance of CD44 in Human Pancreatic Cancer: I. High Expression of CD44 in Human Pancreatic Adenocarcinoma. *Pancreas* **1994**, *9*, 748−752.

(66) Yadav, V. K.; Ryu, J.-H.; Suda, N.; Tanaka, K. F.; Gingrich, J. A.; Schütz, G.; Glorieux, F. H.; Chiang, C. Y.; Zajac, J. D.; Insogna, K. L.; Mann, J. J.; Hen, R.; Ducy, P.; Karsenty, G. Lrp5 Controls Bone Formation by Inhibiting Serotonin Synthesis in the Duodenum. *Cell* *135*, 825−837.

(67) Qhattal, H. S. S.; Liu, X. Characterization of CD44-Mediated Cancer Cell Uptake and Intracellular Distribution of Hyaluronan-Grafted Liposomes. *Mol. Pharmaceutics* **2011**, *8*, 1233−1246.

(68) Sun, H.; Benjaminsen, R. V.; Almdal, K.; Andresen, T. L. Hyaluronic Acid Immobilized Polyacrylamide Nanoparticle Sensors for CD44 Receptor Targeting and pH Measurement in Cells. *Bioconjugate Chem.* **2012**, *23*, 2247−2255.